AIMS Bioengineering, 7(1): 43–54.
DOI: 10.3934/bioeng.2020004
Received: 14 January 2020
Accepted: 12 March 2020
Published: 16 March 2020

http://www.aimspress.com/journal/Bioengineering

Research article

Cell growth on electrospun nanofiber mats from polyacrylonitrile (PAN) blends

Daria Wehlage[1], Hannah Blattner[1], Al Mamun[1], Ines Kutzli[2], Elise Diestelhorst[1], Anke Rattenholl[1], Frank Gudermann[1], Dirk Lütkemeyer[1] and Andrea Ehrmann[1,*]

[1] Faculty of Engineering and Mathematics, Bielefeld University of Applied Sciences, Bielefeld, Germany
[2] Institute of Food Science and Biotechnology, Department of Food Physics and Meat Science, University of Hohenheim, Stuttgart, Germany

* **Correspondence:** Email: andrea.ehrmann@fh-bielefeld.de; Tel: +4952110670254; Fax: +495211067190.

Abstract: Nanofiber mats can be produced by electrospinning from diverse polymers and polymer blends as well as with embedded ceramics, metals, etc. The large surface-to-volume ratio makes such nanofiber mats a well-suited substrate for tissue engineering and other cell growth experiments. Cell growth, however, is not only influenced by the substrate morphology, but also by the sterilization process applied before the experiment as well as by the chemical composition of the fibers. A former study showed that cell growth and adhesion are supported by polyacrylonitrile/gelatin nanofiber mats, while both factors are strongly reduced on pure polyacrylonitrile (PAN) nanofibers. Here we report on the influence of different PAN blends on cell growth and adhesion. Our study shows that adding ZnO to the PAN spinning solution impedes cell growth, while addition of maltodextrin/pea protein or casein/gelatin supports cell growth and adhesion.

Keywords: electrospinning; nanofiber mat; autoclaving; cell growth; adherent cells; CHO cells; DMSO

1. Introduction

Electrospinning is a simple method to prepare nanofiber mats from diverse polymers and polymer blends [1–3]. Several polymers can be electrospun from aqueous solutions, making the

spinning process itself relatively simple and environmentally-friendly, but necessitating a subsequent crosslinking step if the nanofiber mats should be used in humid environments [4–6]. Most waterproof polymers have to be spun from toxic or corrosive solvents, while only some can also be electrospun from low-toxic solvents like dimethyl sulfoxide (DMSO) [7]. Being spinnable from DMSO is one of the reasons why polyacrylonitrile (PAN) is often used in electrospinning [8–10]. Another reason is the possibility to use PAN as a precursor for carbon nanofibers [11–13].

Nanofiber mats are applicable in a broad range of engineering and science areas, e.g. for air or water filtration [14–16], batteries and solar cells [17–19], biotechnology and medical purposes [20–25]. Although most eukaryotic cell culture bioprocesses consist of the cultivation of cells in suspension, certain processes involve the cultivation of adherent cell lines and primary cells. These bioprocesses cover the production of viral vaccines and viral vectors for gene therapy and oncology as well as regenerative medicine or recombinant protein production. The cultivation of adherent cells can be carried out in classical roller bottles or multilayer cell culture trays. However, production costs are relatively high [26].

Microcarriers and hollow fibers represent an alternative to these systems since they allow their implementation in bioreactor systems [27,28]. They can be made of various polymers [29,30]. Modern single use fixed bed bioreactors enable batch to batch constant product quality which is indispensable in pharma processes. Continuous bioprocessing allows for smaller production volumes and higher product concentration. These ready-to-use bioreactors are filled with non-woven macroporous carriers or rolled membranes. The fabric is often made of polyethylene-terephtalate (PET) microfibers which are surface-treated to render them hydrophilic and biocompatible for cell attachment [31–33].

In contrast, nanofibers display fiber diameters that are a hundred times smaller. The development of microcarriers that consist of nanofibers could lead to even higher cell densities in adherent cell culture bioprocesses. Pure PAN nanofibers are known to prevent cell adhesion. Blending PAN with certain additives could improve cell binding [34]. Blends were chosen which showed in pre-tests good morphological stability under oxidative stabilization and carbonization which can be used to make such nanofiber mats conductive. Electroconductive fibers present interesting substrates for myocardial and neural tissue engineering [35–37].

Here we report on cell growth on different nanofiber mats electrospun from pure PAN and PAN blends, thus modifying chemistry and morphology of the fibers in different ways. On the one hand, we used ZnO, an inorganic, heat stable compound which is typically used in dye-sensitized solar cells or photocatalytic degradation of dyes [13]. The second blend partner is maltodextrin, a carbohydrate, combined with pea protein, which can be used in the food industry [38]. Finally, first tests were performed combining milk casein, a globular protein which is used in cheese or as food additive [39], and gelatin which was used in the previous test [34].

Since the previous study underlined the strong influence of the sterilization process [34], all nanofiber mats were autoclaved. Experiments were performed with adherent Chinese hamster ovary (CHO) cells which are often used to produce therapeutic proteins as well as in general biotechnological investigations [40–42] and are thus a typical model system for these tests.

2. Materials and methods

2.1. Nanofiber mats

Nanofiber mats were produced with the needleless electrospinning machine “Nanospider Lab” (Elmarco, Liberec, Czech Republic), using the following spinning parameters: high voltage 80 kV, nozzle diameter 0.8 mm, carriage speed 100 mm/s, substrate speed 0 mm/min (static), ground-substrate distance 240 mm, electrode-substrate distance 50 mm, relative humidity in the spinning chamber 33%, temperature 22 °C.

For the spinning solutions, X-PAN (Dralon, Dormagen, Germany) was dissolved in DMSO (min. 99.9%, S3 Chemicals, Bad Oeynhausen, Germany) by stirring for 2 h at room temperature. Some of the spinning solutions were blended with ZnO (nano powder < 100 nm particle size, Sigma-Aldrich, Germany), casein (according to Hammersten) and gelatin (Abtei, Marienmünster, Germany). These blends were found to result in larger fiber diameters than pure PAN nanofiber mats and thus to retain their morphology and their mechanical properties better during stabilization and carbonization [13,34,39]. In addition, a maltodextrin/protein blend was added which was prepared as follows: 0.63 g of pea protein isolate (Pisane C9, Cosucra, Pecq, Belgium) (corresponds to a protein mass of 0.5 g) was mixed with 8 g maltodextrin with dextrose equivalent (DE) 2 (Eliane MD 2, Avebe, Veendam, Netherlands) and with 1 g maltodextrin with DE 21 (Glucidex 21 D, Roquette, Lestrem, France) [38]. Table 1 gives an overview of different samples under examination. Overall masses of the spinning solutions always add up to 10 g.

Table 1. Samples under examination, indicating the spinning solution and whether samples were also investigated after carbonization.

Sample name	PAN mass/g	ZnO mass/g	Maltodextrin/ pea protein mass/g	Casein mass/g	Gelatin mass/g	DMSO mass/g	Also carbon.
PAN	1.6					8.4	Yes
PAN/ZnO	1.5	0.5				8.0	Yes
PAN/MP	1.5		0.75			7.75	Yes
PAN/CG	1.3			0.1	0.1	8.5	No

Some of the samples were additionally carbonized since many studies reveal advantages of cell growth and orientation on conductive nanofiber substrates [35–37]. These samples were firstly stabilized in a muffle oven B150 (Nabertherm, Lilienthal, Germany) for 1 h at a temperature of 280 °C, approached with a heating rate of 1K/min. Afterwards they were carbonized in a furnace CTF 12/TZF 12 (Carbolite Gero, Neuhausen, Germany) for 1 h at 500 °C, approached with a heating rate of 10 K/min in a nitrogen flow of 150 ml/min.

2.2. Investigations

Images of the nanofiber mat were taken with a confocal laser scanning microscope (CLSM) VK-8710 (Keyence, Neu-Isenburg, Germany), using a nominal magnification of 2000×.

Nanofiber diameters were calculated from 100 fibers per sample using the software ImageJ 1.51j8 (from National Institutes of Health, Bethesda, MD, USA) which was also applied for

fast Fourier transform (FFT) evaluations. Such FFT images show radially diffuse patterns for non-aligned fibers, while oriented fibers can be identified by single lines in the FFT images [43,44].

2.3. Cell growth

Dulbecco's Modified Eagle's medium (DMEM)/Ham's Nutrient Mixture F12 (1:1 DMEM/F12) (SAFC Biosciences, Irvine, UK) was used as a base for cell cultivation. Glucose (Roth, Karlsruhe, Germany) and L-glutamine (Applichem, Darmstadt, Germany) were added to reach a final concentration of 4 g/L and 4 mM, respectively. After setting the pH value to 7.4, the medium was sterile filtered (Sartolab P, 0.45 µm/0.22 µm, Sartorius, Göttingen, Germany). Subsequently, 10% sterile donor horse serum (biowest, Nuaillé, France) were added.

CHO DP-12 cells for this study (LGC Standards GmbH, Wesel, Germany; ATCC no. CRL-12445) grow in vitro to form a monolayer if using a serum containing medium.

Before cell growth experiments, the nanofiber mats were washed three times with highly purified water. Nanofiber mats of 2 cm × 2 cm were glued with Elastosil E41 RTV-1 silicone rubber (Wacker, Burghausen, Germany) on cover slips (21 mm × 26 mm) (Carl Roth, Karlsruhe, Germany) to keep them inside the medium during cultivation. 24 h after gluing, they were washed with water and left for drying in air for another 24 h. Afterwards they were sterilized by autoclaving for 20 min at 121 °C in a VX-75 autoclave (Systec, Linden, Germany) and then placed in 6-well plates (Labsolute, Th. Geyer, Renningen, Germany) inside a safety cabinet Safe 2020 (Thermo Electron LED GmbH, Langenselbold, Germany). Into each well 5 ml medium with 20,000 cells were pipetted. Cultivation was carried out during 4 days (96 h) in a HERAcell 240i incubator (Thermo Electron LED GmbH, Langenselbold, Germany) at 37 °C and 7.5% CO_2.

After cultivation, the medium was pipetted out of the wells, and 1.5 ml glyoxal solution was added to fix the cells [45]. 3 vol% glyoxal solution (containing 34 ml highly purified water, 9.5 ml ethanol (abs., VWR BDH Prolabo, Langenfeld, Germany), 3.75 ml 40% glyoxal (Roth, Karlsruhe, Germany) and 0.36 ml acetic acid p.a. (VWR BDH Prolabo, Langenfeld, Germany)) with a pH value between 4 and 5 were used for this. The well plate was then cooled on ice for 30 min and afterwards incubated for 30 min at room temperature before the glyoxal solution was pipetted out of the wells. Afterwards the nanofiber mats were washed with phosphate buffered saline for 5 min and another 5 min with highly purified water. Subsequently, the cells were dyed with hematoxylin eosin (H&E) Fast Staining Kit (Roth, Karlsruhe, Germany). The dyeing was based on the protocol by Roth. At first the samples were incubated in H&E solution 1 (modified hematoxylin solution) for 6 min. After the incubation, the samples were washed with tap water for 10 s and then with 0.1% hydrochloric acid for 10 s. For bluing, the samples were washed again with tap water for another 6 min. Finally the samples were incubated in H&E solution 2 (modified eosin yellow solution) for 30 s and for another 30 s washed with tap water. The nanofiber mats were taken out and dried in the air.

For the quantitative cell growth investigation, a Cedex^{TM} MS20C cell counter (Innovatis, Bielefeld, Germany) was used. After washing the nanofiber mats with PBS (phosphate-buffered saline), they were treated with a sterile trypsin/EDTA (ethylenediamine tetraacetic acid) solution (biowest, Nuallié, France), resulting in cell detachment. Trypsinization was stopped by diluting the fluid with culture medium in a ratio of 1:10 after incubation at 37 °C for 5 min. 1 ml cell suspension were automatically mixed with 1 ml trypan blue (a vital stain coloring dead cells blue). The cell counter measures dead and living cells with an accuracy of ±5% [46].

All experiments were verified in subsequent, independent test series to avoid possible contaminations or other undesired environmental influences.

3. Results and discussion

Firstly, Figure 1 depicts CLSM images of nanofiber mats after sterilization, revealing the influence of the blending materials. In all cases, the fiber diameters become larger than those of pure PAN nanofibers where the spinning parameters used here resulted in a diameter distribution of (144 ± 40) nm [47]. The diameter distributions for the samples depicted in Figure 1 as well as the FFT evaluations are presented in Figure 2.

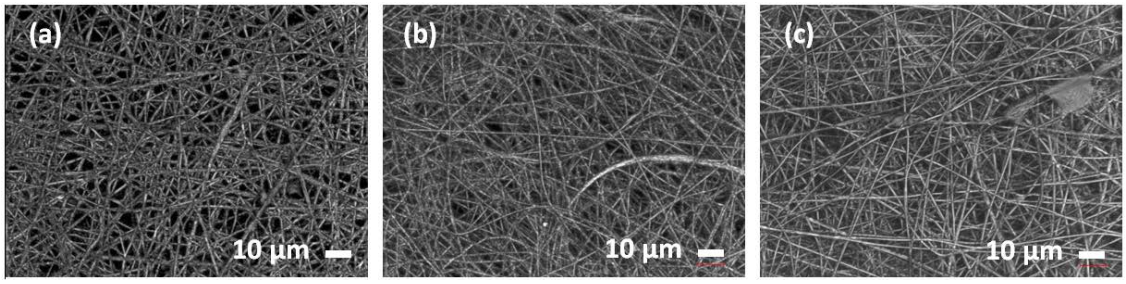

Figure 1. Nanofiber mats from PAN/ZnO (a), PAN/MP (b) and PAN/CG (c).

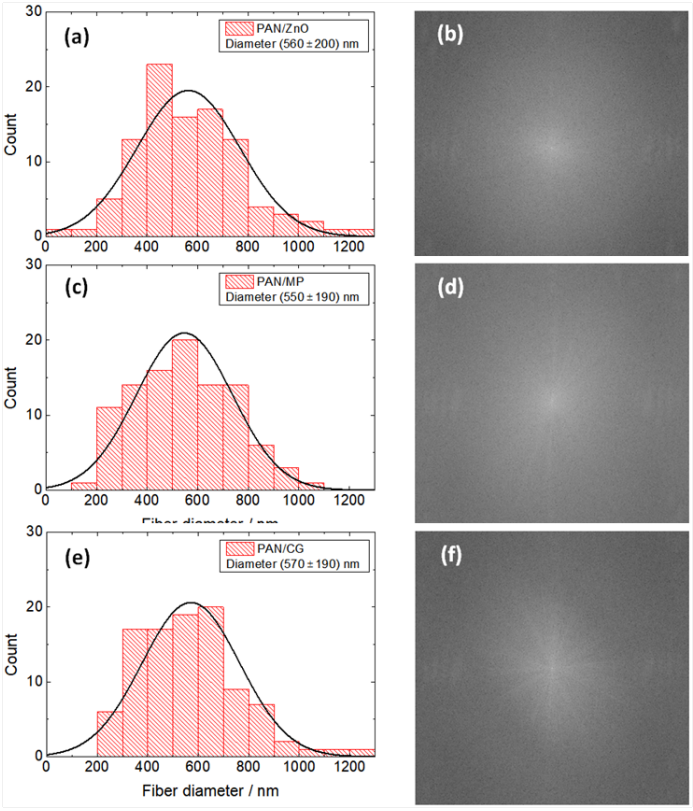

Figure 2. Diameter distributions (left panels) and FFT evaluations (right panels) of nanofiber mats prepared from different PAN blends.

All nanofiber mats show very similar average nanofiber diameters and standard deviations, approximately 4× the average fiber of pure PAN fibers [47]. This effect was also found in the previous investigation of cell growth on PAN/gelatin nanofiber mats [34].

The FFT analysis shows radially diffuse patterns, indicating non-aligned fibers [43]. Future experiments should be made on aligned fibers [44] to investigate differences in cell growth due to a possible fiber orientation in the substrate.

Figure 3 depicts CLSM images of dyed CHO cells adhered on a cover slip in different magnifications. The shape of the adhered cells is similar to long, stretched lenses, while the dead or not adhered ones are round. In this way, optical differentiation is possible between the states before fixation of the cells grown on nanofiber mats.

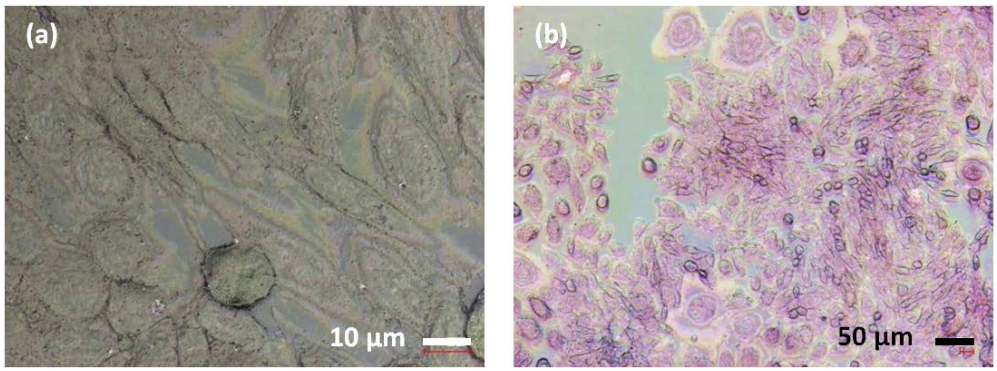

Figure 3. CHO cells adhered on glass cover slips in different magnifications.

The results of cultivation of CHO cells on pure PAN nanofiber mats (as spun and carbonized) are shown in Figure 4. Generally, the hematoxylin eosin staining shows cell nuclei (and other acidic structures) in blue or brown color, depending on the pH value of the dye solution, while basic structures (such as the cytoplasm) are depicted in red. It should be mentioned that images taken on the (black) carbonized nanofiber mats can show reduced or shifted colors, as usual on dark undergrounds.

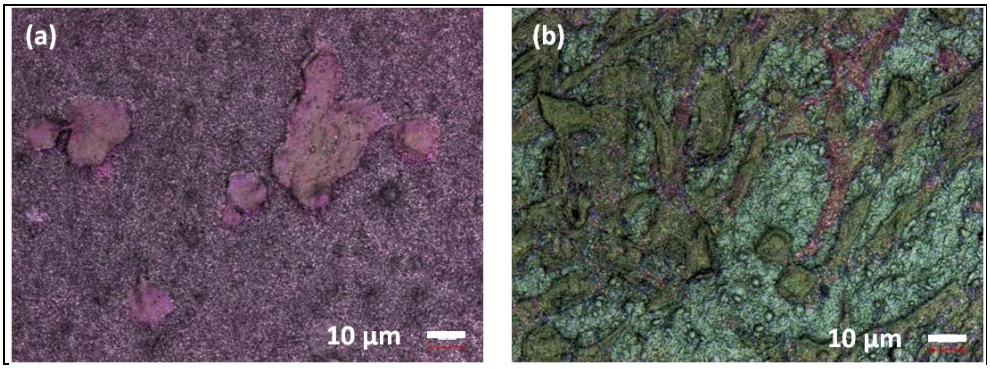

Figure 4. CHO cells on pure PAN nanofiber mats, electrospun (a) and carbonized (b).

While in some areas of the electrospun PAN nanofiber mat, only nuclei are visible, other areas show also living, adhered cells (Figure 4a). For the carbonized PAN nanofiber mat, besides the

brown cell nuclei, also reddish cytoplasm is visible, and the lens-shaped typical form of adhered CHO cells becomes partly visible, while again other cells seem to be dead (Figure 4b). Nevertheless, cell proliferation on this carbon nanofiber mat seems reduced as compared to cell growth, e.g., on PAN/gelatin nanofiber mats [34].

Next, PAN/ZnO nanofiber mats were tested as substrates are shown in Figure 5. While a slight pink undertone is visible in the raw nanofiber mat, probably due to staining of the ZnO by eosin yellow, neither cell nuclei nor cytoplasm can be recognized in both images. This is in contrast to the earlier experiments on PAN/gelatin nanofiber mats which also had increased fiber diameters and showed good cell adhesion and proliferation [34].

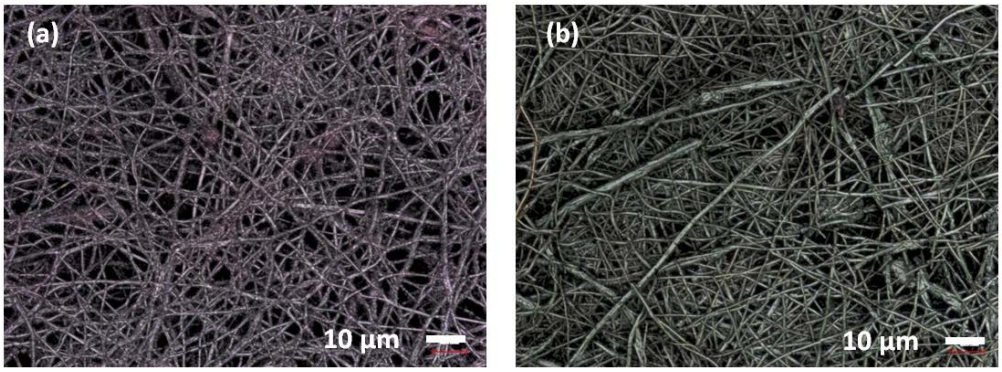

Figure 5. No adherent CHO cells visible on PAN/ZnO nanofiber mats, electrospun (a) and carbonized (b).

This finding indicates that ZnO is a problematic blending partner for cell growth experiments on nanofiber mats. Indeed ZnO nanoparticles are known to have cytotoxic effects, although differences are reported for different cell lines [48–51] which may also suppress the growth of CHO cells on PAN/ZnO nanofiber mats. Since ZnO is not decomposed at a temperature of 500 °C, it stays inside the carbonized nanofiber mats so that its negative impact on cell growth and adhesion persists.

This is opposite for the PAN/MP nanofiber mats depicted in Figure 6. On both the original and the carbonized PAN/MP nanofiber mats, cell adhesion and proliferation are visible. Apparently, similar to the PAN/gelatin nanofiber mats in the previous study, the chemical composition of these nanofiber mats supports cell growth and adhesion.

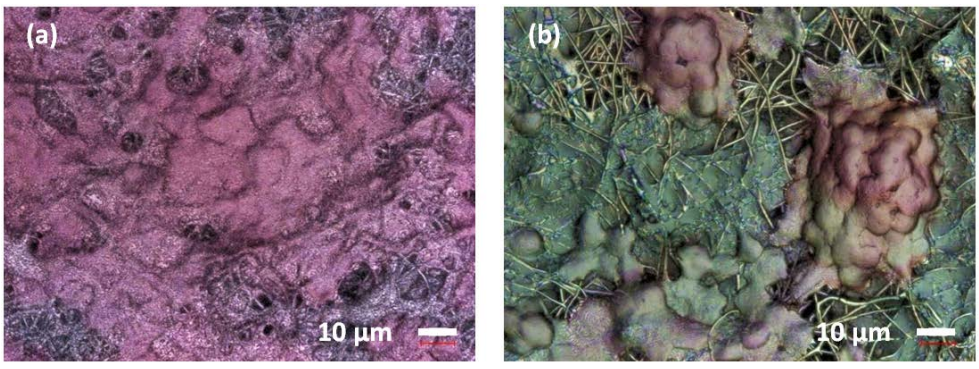

Figure 6. CHO cells on PAN/MP nanofiber mats, electrospun (a) and carbonized (b).

Figure 7 shows first results on newly developed PAN/CG nanofiber mats [38] which will be investigated more in detail in the near future. Unlike PAN/MP or PAN/gelatin [34] nanofiber mats, here the mat morphology changes stronger during autoclaving and the following cultivation procedures. This suggests testing different sterilization methods, such as ozone or UV irradiation, to avoid thermal damages of the nanofiber mats. On the other hand, nanofiber mats with smaller amounts of biopolymers should be tested to enable autoclaving without too strong changes in the fiber structures.

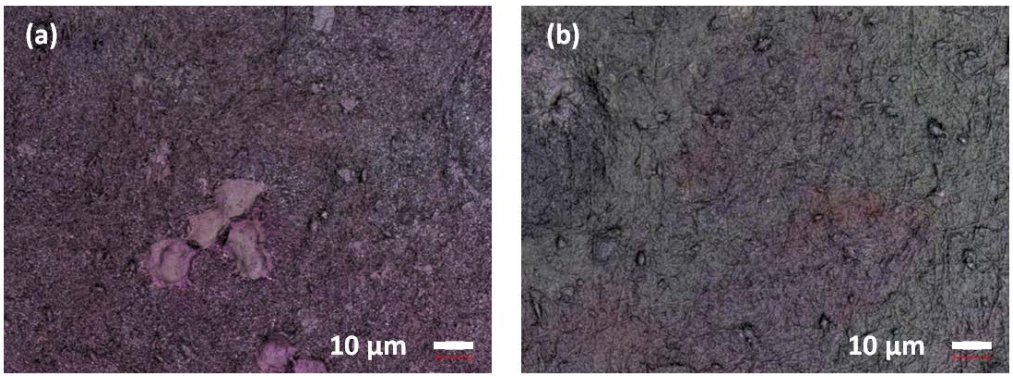

Figure 7. CHO cells on PAN/CG nanofiber mats.

Finally, to underline the aforementioned qualitative findings, the results of the quantitative study are given in Figure 8.

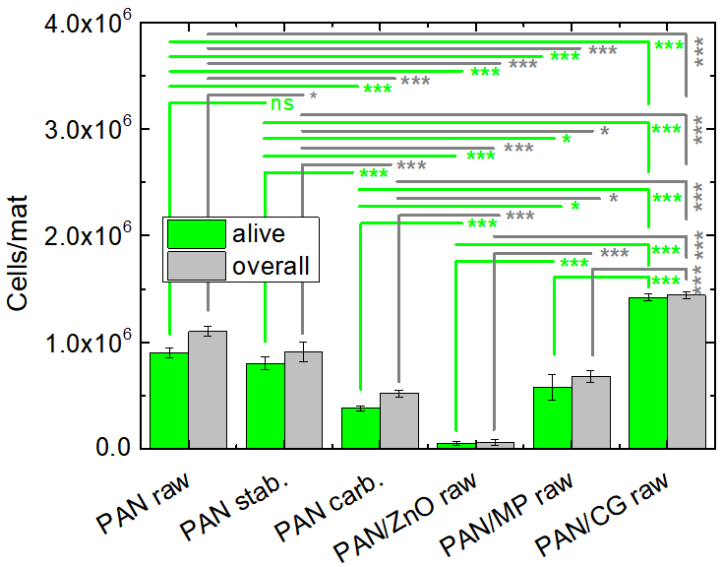

Figure 8. Numbers of CHO cells on diverse nanofiber mats (raw, stabilized or electrospun). Significance levels of $p < 0.05$, $p < 0.01$ and $p < 0.001$ are marked with *, **, and ***, respectively.

Figure 8 clearly shows that PAN/ZnO is not suitable for growth of CHO cells, while PAN/CG shows the best results in terms of cells per nanofiber mat as well as in terms of viability (number of

living cells per overall cells), while the CLSM images showed thicker cell agglomerations for PAN/MP nanofiber mats.

To statistically analyze the results, a one-way ANOVA was used. Homogeneity of variance was verified by Levine's test. The Bonferoni method was used for the comparison of means. For the numbers of living cells, only the comparison of the samples PAN and PAN stab. show no significant difference, while comparing the overall numbers of cells shows significantly differing pairs in all cases.

4. Conclusion

Comparing the nanofiber mats under investigation, it can be stated that PAN/ZnO is not suitable for cell growth, although the ZnO nanoparticles can be expected to be mainly located inside the fibers without contact to the environment [13]. On pure PAN, used after electrospinning, stabilization and carbonization, some cell growth and adhesion were observed, opposite to a previous investigation [34]. The PAN/CG nanofiber mats were stronger influenced by the preparation process, including autoclaving, which resulted in a fully modified morphology most probably due to denatured casein and molten gelatin during heat treatment. Nevertheless, they enabled cell growth and adhesion. The best cell proliferation and adhesion, however, comparable to PAN/gelatin nanofiber mats [34], was found in PAN/CG nanofiber mats. In the next steps, both these nanofiber blends should be optimized by additional studies of cell proliferation for different blend ratios and compared to further experiments on PAN/gelatin nanofiber mats to find the ideal growth conditions for the CHO DP-12 cells.

The utilization of the blended PAN nanofibers as microcarriers in batch and continuous bioprocessing will be evaluated. Moreover, the electroconductivity of carbonized and non-treated blended PAN nanofibers will be investigated to assess their suitability as scaffolds for neural and myocardial tissue engineering.

Acknowledgment

This study was partly funded by the PhD funds and the HiF funds of Bielefeld University of Applied Sciences.

Conflict of interest

All authors declare no conflicts of interest in this paper.

References

1. Dizge N, Shaulsky E, Karanikola V (2019) Electrospun cellulose nanofibers for superhydrophobic and oleophobic membranes. *J Membr Sci* 590: 117271.
2. Pavlova ER, Bagrov DV, Monakhova KZ, et al. (2019) Tuning the properties of electrospun polylactide mats by ethanol treatment. *Mater Des* 181: 108061.

3. Wang JN, Zhao WW, Wang B, et al. (2017) Multilevel-layer-structured polyamide 6/poly(trimethylene terephthalate) nanofibrous membranes for low-pressure air filtration. *J Appl Pol Sci* 134: 44716.
4. Cooper A, Oldinski R, Ma H Y, et al. (2013) Chitosan-based nanofibrous membranes for antibacterial filter applications. *Carbohyd Polym* 92: 254–259.
5. Banner J, Dautzenberg M, Feldhans T, et al. (2018) Water resistance and morphology of electrospun gelatine blended with citric acid and coconut oil. *Tekstilec* 61: 129–135.
6. Grimmelsmann N, Homburg SV, Ehrmann A (2017) Electrospinning chitosan blends for nonwovens with morphologies between nanofiber mat and membrane. *IOP Conf Series Mater Sci Eng* 213: 012007.
7. Wortmann M, Freese N, Sabantina L, et al. (2019) New polymers for needleless electrospinning from low-toxic solvents. *Nanomater* 9: 52.
8. Krasonu I, Tarassova E, Malmberg S, et al. (2019) Preparation of fibrous electrospun membranes with activated carbon filler. *IOP Conf Series Mater Sci Eng* 500: 012022.
9. Plamus T, Savest N, Viirsalu M, et al. (2018) The effect of ionic liquids on the mechanical properties of electrospun polyacrylonitrile membranes. *Polym Test* 71: 335–343.
10. Sabantina L, Mirasol JR, Cordero T, et al. (2018) Investigation of needleless electrospun PAN nanofiber mats. *AIP Conf Proc* 1952: 020085.
11. Wang JH, Cai C, Zhang ZJ, et al. (2020) Electrospun metal-organic frameworks with polyacrylonitrile as precursors to hierarchical porous carbon and composite nanofibers for adsorption and catalysis. *Chemosphere* 239: 124833.
12. de Oliveira JB, Guerrini LM, dos Santos Conejo L, et al. (2019) Viscoelastic evaluation of epoxy nanocomposite based on carbon nanofiber obtained from electrospinning processing. *Polym Bull* 76: 6063–6076.
13. Trabelsi M, Mamun A, Klöcker M, et al. (2019) Increased mechanical properties of carbon nanofiber mats for possible medical applications. *Fibers* 7: 98.
14. Wang L, Zhang C, Gao F, et al. (2016) Needleless electrospinning for scaled-up production of ultrafine chitosan hybrid nanofibers used for air filtration. RSC Adv 6: 105988–105995.
15. Roche R, Yalcinkaya F (2018) Incorporation of PVDF nanofibre multilayers into functional structure for filtration applications. *Nanomater* 8: 771.
16. Lv D, Wang RX, Tang GS, et al. (2019) Ecofriendly electrospun membranes loaded with visible-light-responding nanoparticles for multifunctional usages: highly efficient air filtration, dye scavenging, and bactericidal activity. *ACS Appl Mater Interfaces* 11: 12880–12889.
17. Fu QS, Lin G, Chen XD, et al. (2018) Mechanically reinforced PVdF/PMMA/SiO_2 composite membrane and its electrochemical properties as a separator in lithium-ion batteries. *Energy Technol* 6: 144–152.
18. Mamun A, Trabelsi M, Klöcker M, et al. (2019) Electrospun nanofiber mats with embedded non-sintered TiO_2 for dye sensitized solar cells (DSSCs). *Fibers* 7: 60.
19. Xue YY, Guo X, Zhou HF, et al. (2019) Influence of beads-on-string on Na-Ion storage behavior in electrospun carbon nanofibers. *Carbon* 154: 219–229.
20. Mamun A (2019) Review of possible applications of nanofibrous mats for wound dressings. *Tekstilec* 62: 89–100.
21. Gao ST, Tang GS, Hua DW, et al. (2019) Stimuli-responsive bio-based polymeric systems and their applications. *J Mater Chem B* 7: 709–729.

22. Aljawish A, Muniglia L, Chevalot I (2016) Growth of human mesenchymal stem cells (MSCs) on films of enzymatically modified chitosan. *Biotechnol Prog* 32: 491–500.
23. Muzzarelli RAA, EI Mehtedi M, Bottegoni C, et al. (2015) Genipin-crosslinked chitosan gels and scaffolds for tissue engineering and regeneration of cartilage and bone. *Mar Drugs* 13: 7314–7338.
24. Klinkhammer K, Seiler N, Grafahrend D, et al. (2009) Deposition of electrospun fibers on reactive substrates for in vitro investigations. *Tissue Eng Part C* 15: 77–85.
25. Yoshida H, Klinkhammer K, Matsusaki M, et al. (2009) Disulfide-crosslinked electrospun poly(γ-glutamic acid) nonwovens as reduction-responsive scaffolds. *Macromol Biosci* 9: 568–574.
26. Chatel A (2019) A brief history of adherent cell culture: where we come from and where we should go. *BioProcess Int* 17: 44–49.
27. Whitford WG, Hardy JC, Cadwell JJS (2014) Single-use, continuous processing of primary stem cells. *BioProcess Int* 12: 26–32.
28. Simon M (2015) Bioreactor design for adherent cell culture. The bolt-on bioreactor project, part 1: volumetric productivity. *BioProcess Int* 13: 28-33.
29. Allan SJ, De Bank PA, Ellis MJ (2019) Bioprocess design considerations for cultured meat production with a focus on the expansion bioreactor. *Front Sus Food Syst* 3: 44.
30. GE Healthcare Life Sciences (2013) Microcarrier Cell Culture, Principles and Methods. Available from: http://www.gelifesciences.co.kr/wp-content/uploads/2016/07/023.8_Microcarrier-Cell-Culture.pdf.
31. Lennaertz A, Knowles S, Drugmand JC, et al. (2013) Viral vector production in the integrity iCELLis single-use fixed-bed bioreactor, from bench-scale to industrial scale. BMC Proc 7(S6): P59.
32. Dohogne Y, Collignon F, Drugmand JC et al. (2019) Scale-X bioreactor for viral vector production. Proof of concept for scalable HEK293 cell growth and adenovirus production, Univercell Application note. Available from: https://www.univercells.com/app/uploads/2019/05/scale-X%E2%84%A2-bioreactor-for-viral-production-Adeno_SFM.pdf.
33. Drugmand JC, Aghatos S, Schneider YJ, et al. (2007) Growth of mammalian and lepidopteram cells on BioNOC® II disks, a novel macroporous microcarrier, In: Smith R, *Cell Technology for Cell Products*, Heidelberg: Springer, 781–784.
34. Wehlage D, Blatter H, Sabantina L, et al. (2019) Sterilization of PAN/gelatin nanofibrous mats for cell growth. *Tekstilec* 62: 78–88.
35. Ghasemi A, Imani R, Yousefzadeh M, et al. (2019) Studying the potential application of electrospun polyethylene terephthalate/graphene oxide nanofibers as electroconductive cardiac patc. *Macromol Mater Eng* 304: 1900187.
36. Nekouian S, Sojoodi M, Nadri S (2019) Fabrication of conductive fibrous scaffold for photoreceptor differentiation of mesenchymal stem cell. *J Cell Physiol* 234: 15800–15808.
37. Rahmani A, Nadri S, Kazemi HS, et al. (2019) Conductive electrospun scaffolds with electrical stimulation for neural differentiation of conjunctiva mesenchymal stem cells. *Artif Organs* 43: 780–790.
38. Kutzli I, Beljo D, Gibis M, et al. (2019) Effect of maltodextrin dextrose equivalent on electrospinnability and glycation reaction of blends with pea protein isolate. *Food Biophysics*.

39. Diestelhorst E, Mance F, Mamun A, et al. (2020) Chemical and morphological modification of PAN nanofiber mats by addition of casein after electrospinning, stabilization and carbonization. *Tekstilec* 63: 38–49.
40. Möller J, Korte K, Pörtner R, et al. (2018) Model-based identification of cell-cycle-dependent metabolism and putative autocrine effects in antibody producing CHO cell culture. *Biotechnol Bioeng* 115: 2996–3008.
41. Wippermann A, Rupp O, Brinkrolf K, et al. (2015) The DNA methylation landscape of Chinese hamster ovary (CHO) DP-12 cells. *J Biotechnol* 199: 38–46.
42. Haredy AM, Nishizawa A, Honda K, et al. (2013) Improved antibody production in Chinese hamster ovary cells by ATF4 overexpression. *Cytotechnology* 65: 993–1002.
43. Bazrafshan Z, Stylios GK (2018) Custom-built electrostatics and supplementary bonding in the design of reinforced Collagen-g-P (methyl methacrylate-co-ethyl acrylate)/nylon 66 core-shell fibers. *J Mech Behav Biomed Mater* 87: 19–29.
44. Storck JL, Grothe T, Mamun A, et al. (2020) Orientation of electrospun magnetic nanofibers near conductive areas. *Materials* 13: 47.
45. Richter KN, Revelo NH, Seitz KJ, et al. (2018) Glyoxal as an alternative fixative to formaldehyde in immunostaining and super-resolution microscopy. *EMBO J* 37: 139–159.
46. Huang LC, Lin W, Yagami M, et al. (2010) Validation of cell density and viability assays using Cedex automated cell counter. *Biologicals* 38: 393–400.
47. Sabantina L, Rodríguez-Cano MA, Klöcker M, et al. (2018) Fixing PAN nanofiber mats during stabilization for carbonization and creating novel metal/carbon composites. *Polymers* 10: 735.
48. Baek M, Kim MK, Cho HJ, et al. (2011) Factors influencing the cytotoxicity of zinc oxide nanoparticles: particle size and surface charge. *J Phys Conf Ser* 304: 012044.
49. Sing S (2019) Zinc oxide nanoparticles impacts: cytotoxicity, genotoxicity, development toxicity, and neurotoxicity. *Toxicol Mech Methods* 29: 300–311.
50. Kuebodeaux RE, Bernazzani P, Nguyen TTM (2018) Cytotoxic and membrane cholesterol effects of ultraviolet irradiation and zinc oxide nanoparticles on Chinese hamster ovary cells. *Molecules* 23: 2979.
51. Zukiene R, Snitka V (2015) Zinc oxide nanoparticle and bovine serum albumin interaction andnanoparticles influence on cytotoxicity *in vitro*. *Colloids Surf B* 135: 316–323.

AIMS Press